BIOCHEMISTRY
including biophysical chemistry & molecular biology
Article

Biochemistry **2010,** *49,* 4147–4158 4147
DOI: 10.1021/bi9021473

Cleavage Site Specificity and Conformational Selection in Type I Collagen Degradation†

Ramon Salsas-Escat,[‡,§,∥] Paul S. Nerenberg,[‡,∥,⊥] and Collin M. Stultz*[,§,∥,#]

[§]*Computational and Systems Biology Initiative,* [∥]*Research Laboratory of Electronics,* [⊥]*Department of Physics, and* [#]*Harvard-MIT Division of Health Sciences and Technology, Department of Electrical Engineering and Computer Science, Massachusetts Institute of Technology, Cambridge, Massachusetts 01239* [‡]*Both authors contributed equally to this work*

Received December 14, 2009; Revised Manuscript Received April 9, 2010

ABSTRACT: Excessive degradation of type I collagen is associated with a variety of human diseases such as arthritis, tumor metastasis, and atherosclerosis. Methods that further our understanding of collagenolysis may therefore provide insights into the mechanism of several important disorders. Prior experiments suggest that cleavage of collagen *in vitro* requires intact full-length collagenase, a multidomain protein containing both a catalytic and a hemopexin-like domain. In this work we demonstrate that type I collagen can be degraded at room temperature, a temperature well below the melting temperature of type I collagen, by collagenase deletion mutants that only contain the catalytic domain of the enzyme. Furthermore, these mutant enzymes hydrolyze the same peptide bond that is recognized by the corresponding full-length enzymes. Hence enzyme specificity at room temperature is achieved without the hemopexin-like domain. We demonstrate that these findings can be explained in light of a conformational selection mechanism that dictates that collagenases preferentially recognize and cleave preformed partially unfolded states of collagen.

Collagen is the most abundant protein in the human body and imparts structural integrity to tissues in its role as the primary component of the extracellular matrix (*1*). Type I collagen, in particular, is the most prevalent of the fibril-forming collagens and is the main constituent of bone, tendon, skin, and other tissues (*2*). The structure of type I collagen is characterized by three polyproline II-like polypeptide chains, consisting of two α1(I) chains and one α2(I) chain, which form a triple helix that is approximately 15 Å in diameter (*3*−*5*). While collagen degradation is a natural process necessary for tissue homeostasis, excessive degradation has been associated with a number of disorders such as arthritis, atherosclerotic heart disease, and tumor metastasis (*2*, *6*−*10*). For example, type I collagen is an important component of atherosclerotic plaques, and excessive degradation of collagen in these plaques can lead to plaque rupture and subsequent myocardial infarctions (*11*). Hence studies that explore the mechanism of collagenolysis are of particular interest.

Collagenases, a subfamily of the matrix metalloproteinase (MMP)[1] family, are capable of cleaving native triple-helical collagen and are typically multidomain enzymes composed of at least a catalytic domain and a hemopexin-like domain that are connected by a linker region (*12*, *13*). Collagenases hydrolyze collagen at unique sites that are characterized by a covalent bond between a glycine residue and a leucine or isoleucine residue, followed by an alanine or leucine residue; i.e., G-[I/L]-[A/L] (*14*). This initial degradation step is an essential part of the mechanism of collagen catabolism in that methods that prevent cleavage at this site can retard the progression of diseases associated with excessive collagen degradation in experimental animal models (*15*−*18*).

There are a number of unanswered questions regarding the mechanism of collagenase-mediated collagen degradation. First, it has long been recognized that the prototypical triple-helical structure of collagen will not fit into the active site of MMPs and that scissile bonds within collagen are not solvent-exposed and are therefore inaccessible to the collagenase active site (*19*, *20*). Consequently, it is thought that collagen must adopt non-triple-helical conformations at the cleavage site in order for collagenolysis to occur (*13*, *14*, *19*, *21*, *22*). Second, while several G-[I/L]-[A/L] triplets can be found in the sequence of type I collagen, only one of them is cleaved by collagenases (*14*, *23*, *24*).

Data obtained from circular dichroism and differential scanning calorimetry experiments suggest that there is considerable heterogeneity in the stability of the triple helix along the collagen chain (*25*). Moreover, NMR studies involving collagen-like model peptides in solution, and molecular dynamics (MD) simulations of collagen-like sequences, suggest that at low temperatures (i.e., temperatures below collagen's melting point) regions of type I collagen near the collagenase cleavage site can adopt conformations that have relatively solvent-exposed scissile bonds (*26*, *27*).

A number of experiments have explored whether collagen can adopt conformations at low temperatures that could, in principle, be recognized and cleaved by proteases. Proteases like pepsin, chymotrypsin, and trypsin have been used in assays for partially unfolded states of collagen (*28*). Early experiments incubated type I collagen with trypsin at 25 °C, and no collagen degradation was observed (*29*). More recent experiments incubated type I collagen with high concentrations of the catalytic domain of MMP8 (CMMP8) at room temperature, and again, no degradation was found (*30*). Similar results have been reported with the catalytic domain of MMP1 (CMMP1) (*19*). If the region near the collagenase cleavage site is able to spontaneously

†This work was supported by National Science Foundation Grant 0745638 and a Burroughs Wellcome Fund Career Award.

*To whom correspondence should be addressed. E-mail: cmstultz@mit.edu. Telephone: (617) 253-4961. Fax: (617) 324-3644.

[1]Abbreviations: MMP, matrix metalloproteinase; CMMP, catalytic domain of an MMP; ODE, ordinary differential equation; EDTA, ethylenediaminetetraacetic acid; AcOH, acetyl hydroxide/acetic acid.

Published on Web 04/15/2010

adopt partially unfolded states in solution that can bind the collagenase cleavage site, then one would expect incubation of the catalytic domain of MMPs with collagen to result in collagenolysis. Since this is not the case, it is difficult to reconcile these latter experimental observations with the aforementioned studies that suggest that type I collagen adopts partially unfolded states in the vicinity of the cleavage site in solution. As a result, these latter degradation experiments support a theory where the collagenase cleavage site does not spontaneously adopt partially unfolded states in solution (at temperatures below collagen's melting temperature), and that collagenolysis involves active unfolding of the collagen triple helix by MMPs. In this formalism the coordinated action of both the catalytic and hemopexin-like MMP domains leads to active unwinding of the triple-helical structure (*13*, *19*, *31*, *32*). In addition, recent data argue that the hemopexin-like domain may also play a role in determining cleavage site specificity by binding to specific secondary sites located near the unique collagenase cleavage site (*33*). Hence it has been argued that the hemopexin-like domain plays an essential role in both exposing the scissile bond and in ensuring that only one potential cleavage site is recognized by the collagenase.

In this work we demonstrate for the first time that the degradation of type I collagen at room temperature, a temperature well below type I collagen's melting temperature, does not require the presence of the MMP hemopexin-like domain. Moreover, peptide bond hydrolysis with MMP mutants that contain only the catalytic domain occurs at the unique collagenase cleavage site and not at other potential cleavage sites. Thus both peptide bond hydrolysis and enzyme specificity are achieved with the catalytic domain alone at room temperature. As full-length enzyme is thought to be necessary for collagenase-mediated unwinding, our data imply that enzyme-mediated unwinding is not required for collagenolysis *in vitro*. We therefore analyze our data in light of a conformational selection model where thermal fluctuations at the cleavage site cause collagen to adopt unfolded conformations that are complementary to the collagenase active site. Overall, our findings suggest that type I collagen can adopt locally unfolded states at room temperature and that collagenolysis occurs when collagenases cleave these locally unfolded states.

MATERIALS AND METHODS

Preparation of Type I Collagen. All experiments were carried out in a reaction buffer containing 100 mM Tris-HCl (VWR International) and 10 mM $CaCl_2$ (Sigma-Aldrich Co,) at pH 7.6. Bovine type I collagen (BD Biosciences) was obtained at 3 mg/mL in 0.012 M HCl.

As purification of type I collagen often results in protein that is contaminated with type III collagen, purchased collagen samples were repurified using differential salt precipitation (*34*−*36*). First, type I collagen was diluted to a concentration of 0.5 mg/mL (1.67 μM) in 0.5 M AcOH. The solution was then dialyzed against low salt buffer (0.1 M NaCl, 50 mM Tris, pH 7.5, at 4 °C) followed by dialysis against a high salt buffer (1.8 M NaCl, 50 mM Tris, pH 7.5, at 4 °C), in which type III collagen preferentially precipitates (*36*). At this point the sample was centrifuged for 30 min at 16000*g*, and the supernatant, containing purified type I collagen, was then dialyzed against reaction buffer. All centrifugations were performed at 4 °C to minimize any heating of the sample that might occur during centrifugation. Purity of the final type I solution was confirmed by running degradation experiments with full-length MMP1. In the repurified samples no type III collagen degradation products were observed.

Enzyme Preparation and Characterization. MMP mutants that only contain the catalytic domains of MMP1 (CMMP1) and MMP8 (CMMP8) were purchased from Enzo Life Sciences. The specific activities of both enzymes were determined by the manufacturer at 37 °C to be 356 units/μg for CMMP8 and 1050 units/μg for CMMP1. To verify that the mutant enzymes retained activity under our experimental conditions, we remeasured the specific activities of CMMP1 and CMMP8 at 25 °C in our reaction buffer. Specific activities were determined using an assay based on the MMP1 colorimetric drug discovery kit from Enzo Lifesciences (BML-AK404-0001) (*37*). In short, a 1 mM solution of 5,5′-dithiobis-(2-nitrobenzoic acid), Ellman's reagent, was prepared in reaction buffer. The enzyme was then incubated in the latter buffer with 100 μM colorimetric thiopeptolide of sequence acetyl-proline-leucine-glycine-(2-mercapto-4-methylpentanoyl)leucine-glycine-*O*-ethyl (*38*) (Enzo Lifesciences BML-P125). This substrate is the same as that used by the manufacturer to measure the enzyme activity at 37 °C. The initial velocity was determined using the slope of the absorbance increase at 412 nm after 3 min, yielding specific activities of 289 units/μg for CMMP8 and 766 units/μg for CMMP1 (1 unit = 100 pmol/min of degradation of the thiopeptolide). Full-length MMP1 (FMMP1) was purchased from Anaspec and was provided in a preserving solution containing 1 mg/mL BSA.

Collagen Degradation Experiments. Degradation experiments were performed at a collagen concentration of 150 μg/mL (0.5 μM). Prior studies suggest that the critical concentration for fibril formation was determined to be around 4 μg/mL at relatively low temperatures and under very different experimental conditions (T = 29 °C, buffer consisting of 20 mM $NaHCO_3$, 117 mM NaCl, 5.4 mM KCl, 1.8 mM $CaCl_2$, 0.81 mM $MgSO_4$, 1.03 mM NaH_2PO_4, 0.01% NaN_3) (*39*). To determine whether collagen at 150 μg/mL (0.5 μM) would remain soluble under our experimental conditions (T = 24 °C, reaction buffer), we assessed the extent of collagen aggregation as a function of time.

The aggregation of type I collagen at room temperature was followed by allowing samples to sit at 150 μg/mL (0.5 μM) for specified periods of time at room temperature, followed by centrifugation at 16000*g* for 4 min. The supernatant was then run on an SDS gel and stained with Coomassie colloidal blue. A similar procedure was followed in a prior work to assess the extent of collagen aggregation as a function of time (*39*). Figure 1 depicts the amount of collagen in the supernatant as a function of time. As the intensity of the collagen bands is constant, no significant aggregation of type I collagen is seen under our experimental conditions.

All degradation reactions were performed at room temperature. The temperature was verified using a calibrated thermometer, and all recorded temperatures were 24 °C. Degradation experiments employed purified type I collagen at a concentration of 150 μg/mL (0.5 μM). All enzymes were incubated with 4-aminophenylmercuric acetate, APMA (Sigma-Aldrich Co.), as previously described (*40*) and mixed with type I collagen to a final concentration of 25 μg/mL (1.2 μM) for CMMP8, 40 μg/mL (2.0 μM) for CMMP1, and 1.7 μg/mL (30 nM) for FMMP1. Reactions were stopped by the addition of SDS−Laemmli buffer (Bio-Rad Laboratories) with β-mercapthoethanol (Sigma-Aldrich Co.) and boiled for 10 min. The degradation

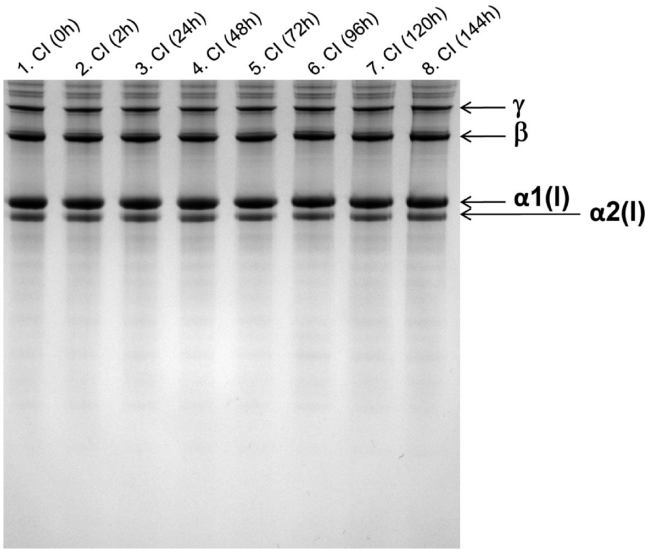

FIGURE 1: Amount of soluble collagen as a function of time. Type I collagen (150 μg/mL, 0.5 μM) was allowed to sit at room temperature for up to 6 days and spun down, and the supernatant was run on SDS−PAGE at each time point.

products were run in 4−12% gradient gels and stained with Coomassie colloidal blue. Gelatin was generated by boiling type I collagen in reaction buffer for 10 min. Gelatin at 150 μg/mL (3 chains × 0.5 μM = 1.5 μM) was then incubated with 13.8 μg/mL (0.67 μM) CMMP8 and 16.6 μg/mL (0.83 μM) CMMP1.

An unstained CMMP8 gel was transferred to a PVDF membrane, which was stained with Coomassie blue. The 1/4 α1 and 1/4 α2 bands were cut from the gels corresponding to the CMMP8 experiments and sent for sequencing to the Tufts University Core Facility, using an ABI 494 protein sequencer. The 1/4 α1 and α2 bands from the CMMP1 reaction could not be sequenced due to the low amount of collagen degraded by CMMP1.

Densitometry Analysis. Densitometry was performed with a Kodak Gel Logic 100 imaging system. Bands were imaged using an automatic lane and band fitting method (Kodak Molecular Imaging software v4.0.0). The percentage of type I collagen degradation by CMMP8 or CMMP1 was measured by dividing the sum of the net intensities of the γ_{deg}, β_{deg}, and 1/4 and 3/4 bands by the sum of the total net intensity of all the bands corresponding to total collagen in a given lane (γ, γ_{deg}, β, β_{deg}, α1, α2, and the 1/4 and 3/4 bands). γ and β bands correspond to N-terminally cross-linked collagen molecules (*41*−*44*). The γ bands correspond to a trimer of chains (*42*, *43*). The β bands correspond to a dimer with two α1 chains (β11) or one α1 and one α2 chain (β12), with only one cross-link (*41*−*43*). These cannot be resolved using the 4−12% gradient gels and were imaged together. Data are presented as the mean and standard deviation over three independent gels per experiment.

Numerical Simulations Using a Conformational Selection Model. We developed a reaction scheme based on a conformational selection model to determine whether our experimental observations could be explained using a formalism that assumes collagen can sample partially unfolded states in solution (*21*). In this scheme collagen exists as an equilibrium distribution between native (N) and partially unfolded, or vulnerable (V), states. The associated equilibrium constant is denoted by K_{eq}. The catalytic domain of MMPs (C) interacts in a nonspecific manner with the native state with binding constant K_{bind}^{NC}, yielding the N·C complex. C can also bind to the vulnerable state, V, with binding constant K_{bind}^{VC}, forming the V·C complex. Binding of C to the native state, N, does not lead to collagenolysis while the V·C complex is degraded with catalytic rate k_{cat}.

This reaction scheme (which is described more fully in the Results section) naturally leads to a set of ordinary differential equations (ODEs), with two rate constants corresponding to each equilibrium/binding constant (i.e., $K_{eq} = k_1/k_2$, $K_{bind}^{NC} = k_{on}^{NC}/k_{off}^{NC}$, and $K_{bind}^{VC} = k_{on}^{VC}/k_{off}^{VC}$). The set of ODEs that describes the time evolution of each species shown is given by

$$\frac{d[N]}{dt} = -k_1[N] + k_2[V] - k_{on}^{NC}[N][C] + k_{off}^{NC}[N\cdot C] \quad (1)$$

$$\frac{d[V]}{dt} = -k_2[V] + k_1[N] - k_{on}^{VC}[V][C] + k_{off}^{VC}[V\cdot C] \quad (2)$$

$$\frac{d[N\cdot C]}{dt} = -k_{off}^{NC}[N\cdot C] + k_{on}^{NC}[N][C] \quad (3)$$

$$\frac{d[V\cdot C]}{dt} = -k_{off}^{VC}[V\cdot C] + k_{on}^{VC}[V][C] - k_{cat}[V\cdot C] \quad (4)$$

$$\frac{d[P]}{dt} = k_{cat}[V\cdot C] \quad (5)$$

$$\frac{d[C]}{dt} = -k_{on}^{NC}[N][C] + k_{off}^{NC}[N\cdot C] - k_{on}^{VC}[V][C] + k_{off}^{VC}[V\cdot C] + k_{cat}[V\cdot C] \quad (6)$$

where P denotes the products of collagenolysis.

We used previously determined rate constants for MMP1 binding to a heterotrimeric collagen-like peptide that contains the type I collagen collagenase cleavage site at a temperature substantially less than its melting temperature (i.e., we expect this peptide to be in a well-folded triple-helical conformation at this temperature) to estimate the native state binding rate constants, k_{on}^{NC} and k_{off}^{NC} ($k_{on}^{NC} = 1.56 \times 10^3$ M^{-1} s^{-1}, $k_{off}^{NC} = 5.35\times10^{-3}$ s^{-1}) (*45*). The catalytic rate constant of the vulnerable state, k_{cat}, for CMMP1 was estimated from the experimentally measured catalytic rates of MMP1 degrading gelatin (*46*). Because k_{cat} measurements do not exist for CMMP8, we set lower and upper bounds for the catalytic rate based on previously published data. The lower bound of k_{cat} for CMMP8 was set equal to that of CMMP1, as it is known that MMP8 has a greater catalytic rate than MMP1 for the same substrate and at the same temperature (*46*, *47*). Upper bounds for the catalytic rate of CMMP8 were obtained from experimentally measured rate constants of FMMP8 degrading linear collagen-like peptides (*48*). This approach yielded a range of k_{cat} for CMMP8 spanning 0.11−11 s^{-1}.

Finding the concentration of each reactant species as a function of time requires knowledge of each of the remaining rate constants, k_1, k_2, k_{on}^{VC}, and k_{off}^{VC}. Previous studies with a related reaction scheme demonstrated that the model is not sensitive to the specific choice of the individual rate constants when one is interested in the reactant concentrations over long time periods (i.e., a time that is long with respect to the individual rate constants themselves) (*21*). In this case, the system behavior is dependent on the ratio of the rate constants or, equivalently, the associated equilibrium and binding constants K_{eq} and K_{bind}^{VC}. Since

our experiments occur over days, which is very long with respect to the folding/unfolding and binding processes of interest, we determined the behavior of the system as a function of K_{eq} and K_{bind}^{VC}.

To convert a given K_{eq} into the appropriate transition rate constants, k_1 and k_2, for the solution of the ODEs, we used initial rate constant values (k_1^{init} and k_2^{init}, set equal to 10^6 s^{-1}) that are consistent with the folding times for a number of small proteins (*49*, *50*). These rate constants were then multiplied by a scale factor α according to

$$\left.\begin{aligned} k_1 &= \alpha^{1/2} k_1^{init} \\ k_2 &= \alpha^{-1/2} k_2^{init} \end{aligned}\right\} K_{eq} = \frac{k_1}{k_2} = \alpha \frac{k_1^{init}}{k_2^{init}}$$

In this way, the appropriate rate constants can be determined for any value of K_{eq}. We use a similar approach to determine the vulnerable state binding rate constants, k_{on}^{VC} and k_{off}^{VC}, from a given K_{bind}^{VC}:

$$\left.\begin{aligned} k_{on}^{VC} &= \beta^{1/2} k_{on}^{VC,init} \\ k_{off}^{VC} &= \beta^{-1/2} k_{off}^{VC,init} \end{aligned}\right\} K_{bind}^{VC} = \frac{k_{on}^{VC}}{k_{off}^{VC}} = \beta \frac{k_{on}^{VC,init}}{k_{off}^{VC,init}}$$

The initial rate constants for binding the vulnerable state, $k_{on}^{VC,init}$ and $k_{off}^{VC,init}$, were set equal to experimentally measured rates for MMP1 binding to a heterotrimeric collagen-like peptide that contains the type I collagen collagenase cleavage site at a temperature substantially greater than its melting temperature (i.e., we expect the triple helix to be mostly unfolded and thus the scissile bonds to be solvent-exposed at this temperature) ($k_{on}^{VC,init} = 4.5 \times 10^2$ M^{-1} s^{-1}, $k_{off}^{VC,init} = 5.94 \times 10^{-3}$ s^{-1}) (*45*). With these rate constants, eqs 1−6 are then solved using the ode15s solver in MATLAB 2008a (MathWorks) using the durations and initial concentrations of collagen and enzyme specific to the relevant degradation experiment(s).

Solutions to the model yield the concentration of collagen degradation products as a function of time, $P_{model}(t)$, while the degradation experiments yield the fraction of peptide/collagen degraded as a function of time, $F_{exp}(t)$. To relate the calculated concentrations to the measured degraded fractions, we normalize the concentration of degradation products to the initial substrate concentration: $F_{model}(t) = P_{model}(t)/S_{init}$, where S_{init} is the initial substrate concentration. We then calculate the root mean square error (RMSE) between experimental and model time courses according to the equation $RMSE = [n^{-1}\sum_{t=1}^{n}(F_{model}(t) - F_{exp}(t))^2]^{1/2}$, where n is the number of experimental time points.

RESULTS

Collagenolysis without a Hemopexin-like Domain. In a prior work we introduced a conformational selection model in which collagen is able to adopt either a well-folded native triple-helical state or a vulnerable state where the region near the collagenase cleavage site is unfolded and solvent exposed (*21*). MMPs can bind to either state, but collagenolysis only occurs when MMPs bind to vulnerable states. The model is based on the premise that collagen adopts different conformations in solution and that collagenolysis occurs when the appropriate conformers are selected by the enzyme. A reexamination of collagen degradation experiments suggests that the failure to observe collagenolysis with MMP deletion mutants, which contain only the catalytic domain, is due to the fact that these mutant enzymes bind partially unfolded states of collagen with reduced affinity relative to the full-length enzyme. A corollary of this result is that collagenolysis could occur if collagen is exposed to relatively high concentrations of mutant enzymes and relatively long incubation times are used (*21*). To test this, we exposed type I collagen to both the catalytic domains of MMP8 and MMP1 (denoted as CMMP8 and CMMP1, respectively).

Bovine type I collagen was incubated with high concentrations of CMMP8 at room temperature, a temperature well below the melting temperature of type I collagen (*51*, *52*). After 48 h type I collagen degradation was observed in solutions containing CMMP8 (Figure 2A, lanes 1−7). Degradation bands exhibit the familiar 3/4 and 1/4 fragments that are associated with cleavage at the unique collagenase cleavage site by the wild-type collagenase MMP1 (FMMP1, Figure 2A, lane 9). N-Terminal amino acid sequencing of the 1/4 α1 and 1/4 α2 bands confirms that the CMMP8 deletion mutant cleaves at the unique cleavage site recognized by the wild-type enzyme (data not shown). To demonstrate that our results are not specific to MMP8, we exposed type I collagen to a deletion mutant containing only the catalytic domain of MMP1 (Figure 2B, lanes 1−5). Despite the fact that higher concentrations of enzyme and longer incubation times were used, type I collagen degradation with CMMP1 was significantly less efficient than that observed with CMMP8. The 1/4 α1 and 1/4 α2 bands from the CMMP1 reaction could not be sequenced due to the low amount of collagen that is degraded by CMMP1. However, the resulting cleavage pattern is the same as that observed with FMMP1 and CMMP8. In bovine type I collagen, the closest potential cleavage sites of sequence G-[I/L]-[A/L] are 48 and 30 residues away from the true cleavage site in the α1 and α2 chains, respectively (*53*−*59*). If these potential sites were cleaved, the pattern of fragments observed would be significantly different from the FMMP1 control, suggesting that CMMP1 mediated cleavage, as in the case of CMMP8, occurs at the same site.

To confirm that our findings are not due to contamination of our collagen samples with unfolded type I collagen chains (gelatin), we incubated CMMP8 and CMMP1 with gelatin. Both CMMP8 and CMMP1 cleave gelatin at several sites, yielding multiple degradation bands on SDS−PAGE (Figure 2A, lane 8, Figure 2B, lane 6) (*19*, *46*). Since these bands are not seen when CMMP8 and CMMP1 are incubated with collagen, contamination of our collagen sample with unfolded collagen chains does not explain our results.

To further demonstrate that our results cannot be explained by contamination of the original collagen sample with low concentrations of full-length MMPs, we incubated solutions of type I collagen containing 4-aminophenylmercuric acetate (APMA), to activate any latent enzyme, but without any added collagenases. SDS−PAGE of the solutions after 6 days of incubation did not exhibit any degradation bands, thereby arguing that contamination with latent enzyme does not explain our findings (Figure 3A). Similarly, to rule out the presence of other contaminating proteases in our CMMP1 and CMMP8 preparations, we incubated type I collagen with CMMP1/8 in the presence of 50 mM EDTA. While EDTA is a known inhibitor of collagenases, it does not affect the activity of nonmetal-dependent proteases (*60*) . No collagen degradation is detected when EDTA is used as an MMP inhibitor, even after 6 days of incubation (Figure 3B). As a further test, we incubated both CMMP1 and CMMP8 with gelatin and EDTA. Since a number of nonmetal-dependent proteases cleave gelatin more readily than collagen, this provides another complementary assay for protease contamination (*61*). These data also did not reveal any evidence of collagen degradation by SDS−PAGE, thereby suggesting that our enzyme preparation

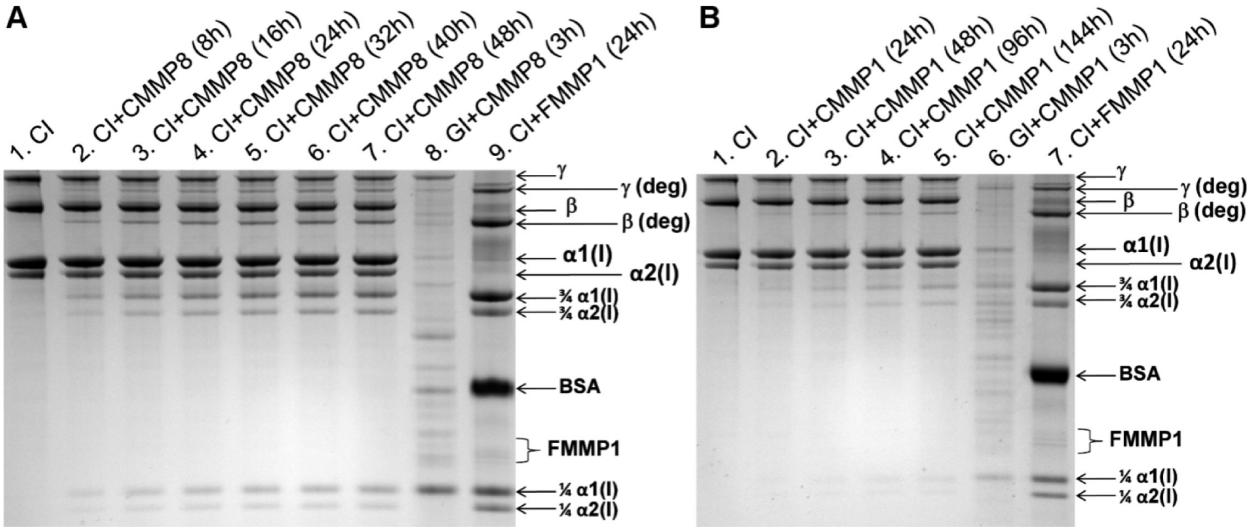

FIGURE 2: Degradation profiles of type I collagen at room temperature with CMMP8 and CMMP1. Intact type I collagen (CI) bands include monomeric α1(I) and α2(I) bands, dimeric β bands, and trimeric γ bands. The β and γ aggregates correspond to N-terminally cross-linked collagen molecules (*41*−*44*). Type I collagen degradation bands include α1(I) and α2(I) 3/4 and 1/4 fragments and degradation of cross-linked chains, β_{deg} and γ_{deg}. (A) Type I collagen incubated with CMMP8. Lane 1: Type I collagen (150 μg/mL, 0.5 μM). Lanes 2−7: Type I collagen (150 μg/mL, 0.5 μM) incubated with the catalytic domain of MMP8 (CMMP8) (25 μg/mL, 1.2 μM) for 8, 16, 24, 32, 40, and 48 h, respectively. Lane 8: Type I collagen gelatin (GI, 150 μg/mL, 1.5 μM) incubated with CMMP8 (13.8 μg/mL, 0.67 μM) for 3 h. Lane 9: Type I collagen (150 μg/mL, 0.5 μM) incubated with full-length MMP1 (FMMP1) (1.7 μg/mL, 30 nM) for 24 h. This lane contains a bovine serum albumin (BSA) band since FMMP1 is supplied in a buffer containing 1 mg/mL BSA. (B) Type I collagen incubated with CMMP1. Lane 1: Type I collagen (150 μg/mL, 0.5 μM). Lanes 2−5: Type I collagen (150 μg/mL, 0.5 μM) incubated with the catalytic domain of MMP1 (CMMP1) (40 μg/mL, 2.0 μM) for 24, 48, 96, and 144 h, respectively. Lane 6: Type I collagen gelatin (GI 150 μg/mL, 1.5 μM) incubated with CMMP1 (16.6 μg/mL, 0.83 μM) for 3 h. Lane 7: Type I collagen (150 μg/mL, 0.5 μM) incubated with full-length MMP1 (FMMP1) (1.7 μg/mL, 30nM) for 24 h. As with lane 9 in (A), this lane contains a BSA band since FMMP1 was supplied in a buffer containing 1 mg/mL BSA.

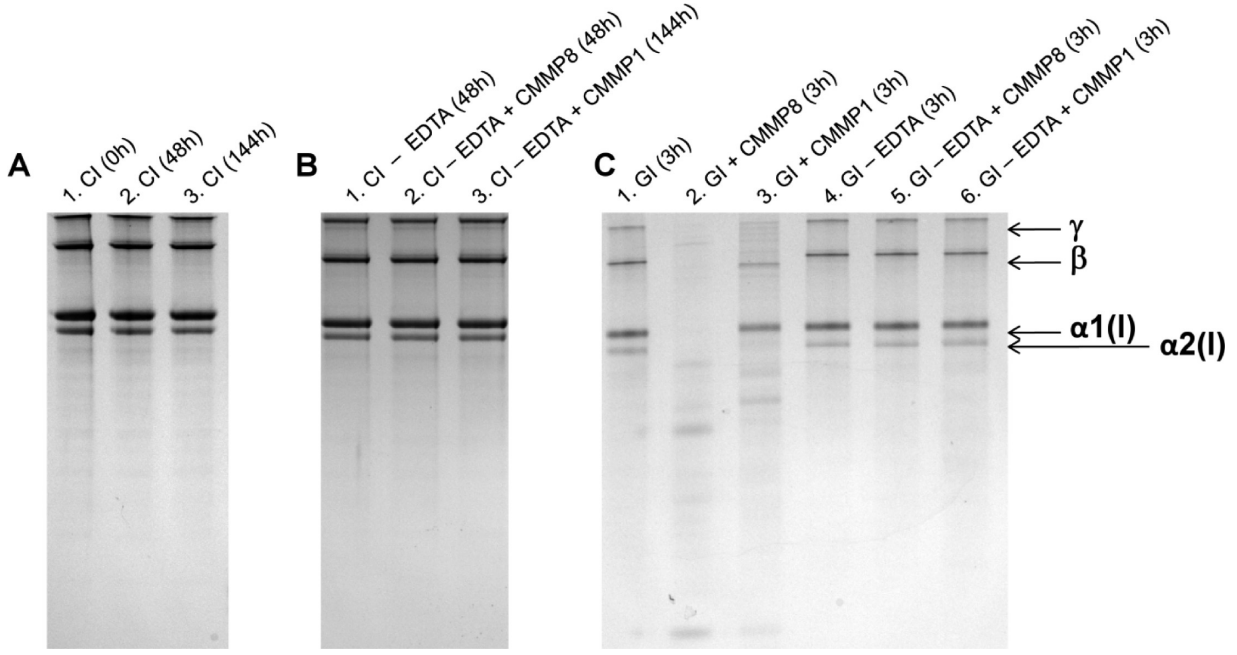

FIGURE 3: Testing for the presence of contaminating MMPs and other proteases. (A) Type I collagen (150 μg/mL, 0.5 μM) incubated in the presence of APMA without the addition of any collagenases for 0, 48, and 144 h. No degradation bands can be observed, which argues that no contaminating MMPs are present. (B) Testing for the presence of contaminating proteases in the CMMP1/8 solutions with collagen. Lane 1: Type I collagen (150 μg/mL, 0.5 μM) in reaction/EDTA buffer in the absence of collagenases incubated for 48 h. Lane 2: Type I collagen (150 μg/mL, 0.5 μM) incubated against CMMP8 (25 μg/mL, 1.2 μM) in reaction/EDTA buffer. Degradation of gelatin cannot be observed. Lane 3: Type I collagen (150 μg/mL, 0.5 μM) incubated against CMMP1 (40 μg/mL, 2.0 μM) in reaction/EDTA buffer. Degradation of collagen cannot be observed. (C) Testing for the presence of contaminating proteases in the CMMP1/8 solutions with gelatin. Lane 1: Type I collagen gelatin (GI 150 μg/mL, 1.5 μM) in reaction buffer in the absence of collagenases incubated for 3 h. Lane 2: Type I collagen gelatin (GI 150 μg/mL, 1.5 μM) incubated against CMMP8 (1.4 μg/mL, 67nM) in reaction buffer. Degradation of gelatin can be observed. Lane 3: Type I collagen gelatin (GI 150 μg/mL, 1.5 μM) incubated against CMMP1 (1.4 μg/mL, 69 nM) in reaction buffer. Degradation of gelatin can be observed. Lane 4: Type I collagen gelatin (GI 150 μg/mL, 1.5 μM) in reaction/EDTA buffer in the absence of collagenases incubated for 3 h. Lane 5: Type I collagen gelatin (GI 150 μg/mL, 1.5 μM) incubated against CMMP8 (1.4 μg/mL, 67nM) in reaction/EDTA buffer. Lane 6: Type I collagen gelatin (GI 150 μg/mL, 1.5 μM) incubated against CMMP1 (1.4 μg/mL, 69 nM) in reaction/EDTA buffer.

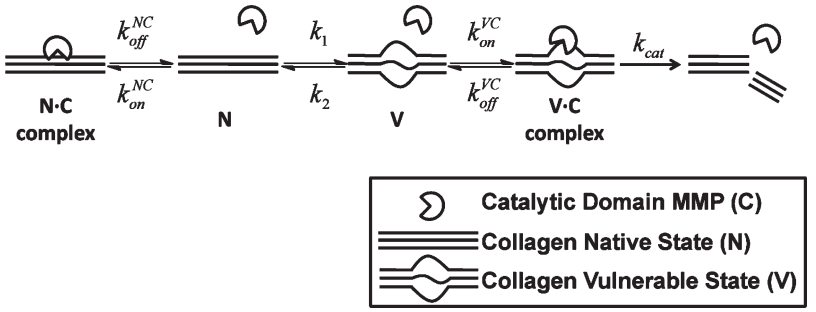

FIGURE 4: A conformational selection mechanism for collagenolysis with MMP catalytic domains. Collagen exists in an equilibrium between native (N) and vulnerable (V) states with the equilibrium determined by $K_{eq} = k_1/k_2$. The catalytic domain of MMPs (C) interacts in a nonspecific manner with the native state with binding constant $K_{bind}^{NC} = k_{on}^{NC}/k_{off}^{NC}$, yielding the N·C complex. C binds to the vulnerable state, V, with binding constant $K_{bind}^{VC} = k_{on}^{VC}/k_{off}^{VC}$, forming the V·C complex. The V·C complex is then degraded with catalytic rate k_{cat}.

does not contain contaminating proteases (Figure 3C). Interestingly, Figure 3C shows that CMMP8 completely cleaves gelatin after 3 h but that CMMP1 preferentially cleaves the α2 chain, a finding that is consistent with prior experimental data on the efficiency of MMP1-mediated degradation of α1(I) and α1(2) chains (*46*).

A Conformational Selection Model for Collagenolysis. Our data demonstrate that peptide bond hydrolysis at the unique collagenase cleavage site can occur *in vitro* at room temperature with only the catalytic domain of MMPs. Since CMMP8 and CMMP1 cleave unfolded collagen at multiple sites (Figure 2A, lane 8, Figure 2B, lane 6) but triple-helical collagen at only one site (Figure 2A, lane 7, Figure 2B, lane 5), we interpret our findings in light of a model where unfolding (due to thermal fluctuations) of collagen at the unique cleavage site enables collagenases to gain access to their corresponding scissile bonds (Figure 4) (*21*). In this model collagen can exist in both native triple-helical (N) and vulnerable states (V), and collagenolysis occurs when the enzyme (consisting of only the catalytic domain, C) binds and cleaves the vulnerable state. Vulnerable states correspond to the ensemble of conformers that have the collagenase cleavage site in an unfolded and solvent-exposed conformation. We use N·C and V·C to denote complexes of the native and vulnerable states, respectively, with the mutant enzyme that only contains the catalytic domain, and P denotes the degradation products released by the enzyme after cleavage.

This reaction scheme naturally leads to a set of ordinary differential equations (ODEs) that can be solved numerically, yielding the concentration of each species as a function of time (see Materials and Methods). Numerical solutions of the ODEs are exact in that they do not make any assumptions about steady-state behavior and they specifically account for the different rate constants associated with each of the different species in the reaction. Generating solutions for the model therefore requires inputs in the form of rate constants associated with each of the various steps in the mechanism.

Previous studies with a related reaction scheme demonstrated that the model is not sensitive to the specific choice of the individual rate constants when one is interested in the reactant concentrations over long times with respect to the individual rate constants themselves (*21*). In this scenario, the solutions to the ODEs depend more on the ratio of the rate constants (*21*). Since our experiments occur over days and theoretical estimates for local unfolding/folding events within the collagen triple helix are on the order of inverse nanoseconds (*20*, *27*), and rate constants for binding reactions in general are on the order of inverse milliseconds (*45*), we explored the behavior of the system as a function of the associated equilibrium and binding constants, $K_{eq} = k_1/k_2$, $K_{bind}^{VC} = k_{on}^{VC}/k_{off}^{VC}$, and $K_{bind}^{NC} = k_{on}^{NC}/k_{off}^{NC}$. It is important to note that while we use these equilibrium/binding constants to describe the behavior of the model, the associated ODEs explicitly depend on the individual rate constants.

As described in Materials and Methods, we estimate K_{bind}^{NC} using previously determined collagenase binding rate constants, which were obtained under conditions when the triple-helical state is expected to be most stable (*45*) (we note, however, that the model is not sensitive to the choice of binding constant for the native state, K_{bind}^{NC} (*21*)). The catalytic rate constant, k_{cat}, corresponds to the rate of peptide bond hydrolysis after the enzyme has bound the unfolded region containing the cleavage site. Bounds for k_{cat} are therefore obtained from experimentally measured rate constants from MMP-mediated degradation of gelatin and unfolded collagen-like peptides (see Materials and Methods) (*46*, *48*). This leaves two undetermined parameters for the model: K_{eq} (the equilibrium constant describing the relative concentration of vulnerable and native conformers) and K_{bind}^{VC} (the binding constant of the catalytic domain for vulnerable states). The method by which K_{eq} and K_{bind}^{VC} are converted into forward/backward and on/off rate constants, respectively, for the numerical simulations is described in Materials and Methods.

To determine estimates for the missing parameters, we fit the ODEs arising from the model shown in Figure 4 to experimental degradation data. We begin by focusing on previous degradation experiments that incubated CMMP8 at room temperature with a heterotrimeric type I collagen-like model peptide that contains the collagenase cleavage site and its surrounding residues (trimer A, Figure 5A) (*45*). The melting temperature of this peptide is 9 °C, and experiments were performed at 25 °C; hence, the peptide is largely unfolded at this temperature. In our model K_{eq} represents the equilibrium constant between native and vulnerable states, where the vulnerable ensemble includes all conformers that have the collagenase cleavage site in an unfolded and solvent-exposed conformation. Consequently, for this system we expect $K_{eq} > 1$, and therefore fitting these data to the model shown in Figure 4 provides a test of the method. Using the reaction scheme outlined in Figure 4, we computed the amount of peptide that would be degraded as a function of time for a range of K_{eq}, $(K_{bind}^{VC})_{CMMP8}$, and k_{cat} values and compared these degradation profiles to the corresponding experimental data. For each triplet (K_{eq}, $(K_{bind}^{VC})_{CMMP8}$, k_{cat}), we computed the root mean square error (RMSE) between the degradation time course obtained with the model and the experimental data (see Materials and Methods). While a relatively wide range of values for K_{eq} and $(K_{bind}^{VC})_{CMMP8}$ were tried ($10^{-6} \leq K_{eq} \leq 10^{6}$,

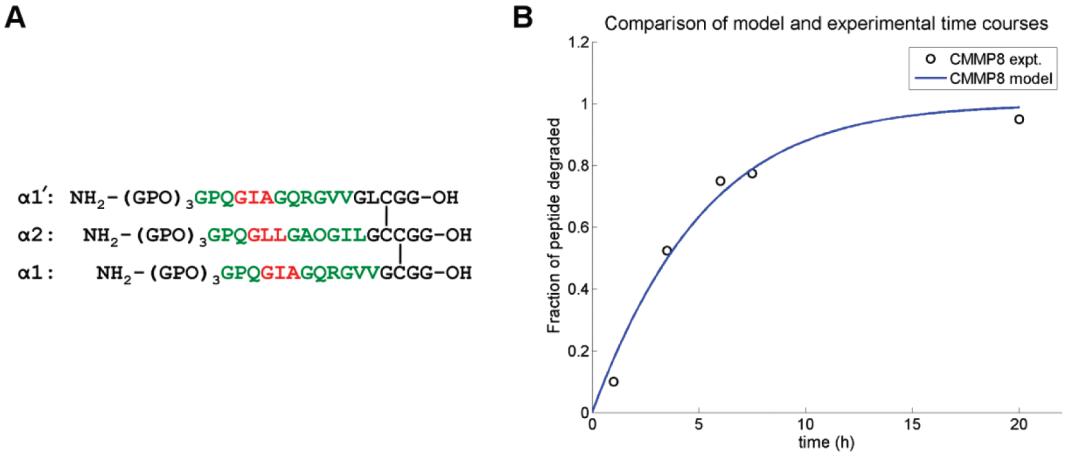

FIGURE 5: Conformational selection and degradation of trimer A by CMMP8. (A) Sequence of the type I collagen-like model peptide trimer A from Ottl et al. used in prior degradation experiments with CMMP8 (*45*). The type I collagen sequence surrounding the collagenase cleavage site is shown in green, while the triplets containing the scissile bonds are indicated in red. The disulfide linkages of the C-terminal cystine knot region are indicated with the black vertical lines. (B) Comparison of model and experimental degradation time courses over 20 h for best fit values $K_{eq} = 60$, $(K_{bind}^{VC})_{CMMP8} = 0.7 \times 10^6\ M^{-1}$, and $k_{cat} = 1.1\ s^{-1}$. Experimental data are indicated by the black circles; the model time course is indicated by the blue line. For these experiments the concentration of trimer A was 50 μM, and the concentration of enzyme was 50 nM.

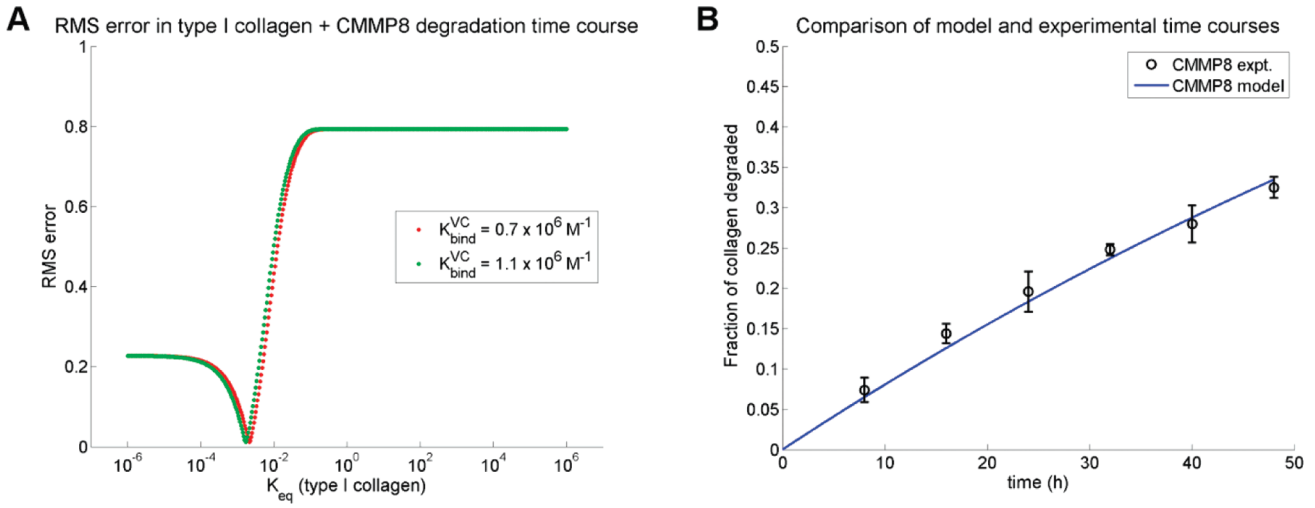

FIGURE 6: Conformational selection and degradation of type I collagen by CMMP8. (A) Root mean square error (RMSE) of the conformational selection model over the time course for degradation experiments utilizing type I collagen and CMMP8. For each value of K_{eq}, the fraction of degraded type I collagen was computed at 8, 16, 24, 32, 40, and 48 h. The root mean square difference was then calculated using these fractions and the experimentally measured fraction of degraded collagen. RMSE curves are computed using the lower (red) and upper (green) bounds of $(K_{bind}^{VC})_{CMMP8}$. (B) A comparison of model and experimental degradation time courses over 48 h for best fit values $K_{eq} = 2.1 \times 10^{-3}$, $(K_{bind}^{VC})_{CMMP8} = 0.7 \times 10^6\ M^{-1}$, and $k_{cat} = 1.1\ s^{-1}$. Experimental data are indicated by the black circles with error bars; the model time course is indicated by the blue line.

$10^0\ M^{-1} \leq (K_{bind}^{VC})_{CMMP8} \leq 10^{12}\ M^{-1}$), the best fits are obtained when $K_{eq} > 30$ and $(K_{bind}^{VC})_{CMMP8} = (0.7-1.1) \times 10^6\ M^{-1}$, regardless of the value of k_{cat} that was used ($0.11\ s^{-1} \leq k_{cat} \leq 11\ s^{-1}$) (Table S1 and Figure S1, Supporting Information). Moreover, varying k_{cat} by 2 orders of magnitude caused the minimum RMSE to vary by only 2%. As the best fits have $K_{eq} > 30$, these results suggest that the vulnerable state of the peptide dominates at room temperature, a finding in agreement with the experimental conditions, as discussed above. Moreover, the predicted results from the model using these values show excellent agreement with experiment (Figure 5B).

Determining K_{eq} for Type I Collagen at Room Temperature. To obtain an estimate for K_{eq} at room temperature, we quantified the extent of collagen degradation over time using the data shown in Figure 2A. We then fit the reaction scheme shown in Figure 4 to these data to obtain an estimate for K_{eq}. We note that the previously discussed studies on a heterotrimeric type I collagen-like peptide, which contains the collagenase scissile bond, found that $(K_{bind}^{VC})_{CMMP8} = (0.7-1.1) \times 10^6\ M^{-1}$. As this peptide is a model for the collagenase cleavage site, we used this range of $(K_{bind}^{VC})_{CMMP8}$ in our numerical calculations of the model for type I collagen.

We again computed the RMSE between the degradation time courses obtained with the model using many different values of K_{eq} and compared these results to the experimentally determined degradation time course. Varying k_{cat} of CMMP8 over 2 orders of magnitude, as we did for the aforementioned model peptide data, did not change the best fit values for K_{eq} and caused the minimum RMSE to again vary by only 2% (Table S2 and Figure S2, Supporting Information). The best fits between the model and experiment are achieved when $K_{eq} = (1.7-2.1) \times 10^{-3}$ (Figure 6A), and the corresponding degradation plot obtained

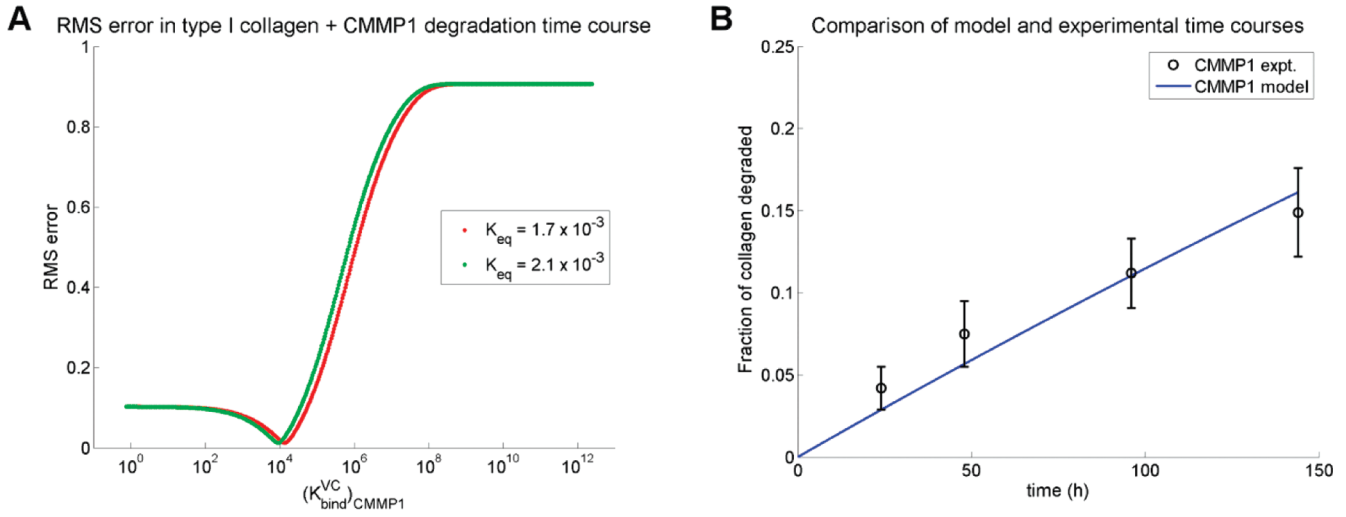

FIGURE 7: Conformational selection and degradation of type I collagen by CMMP1. (A) RMSE of the conformational selection model over the time course for degradation experiments utilizing type I collagen and CMMP1. For each value of $(K^{VC}_{bind})_{CMMP1}$, the fraction of degraded type I collagen was computed at 24, 48, 96, and 144 h. The root mean square difference was then calculated using these fractions and the experimentally measured fraction of degraded collagen. RMSE curves are computed using the lower (red) and upper (green) bounds of K_{eq}. (B) A comparison of model and experimental degradation time courses over 48 h for best fit values $K_{eq} = 2.1 \times 10^{-3}$, $(K^{VC}_{bind})_{CMMP1} = 0.9 \times 10^4$ M^{-1}, and $k_{cat} = 0.11$ s^{-1}. Experimental data are indicated by the black circles with error bars; the model time course is indicated by the blue line.

from the model agrees well with experiment (Figure 6B). This value for K_{eq} suggests that the folded triple-helical native state is more favorable at room temperature.

Determining K^{VC}_{bind} for CMMP1. Despite the fact that CMMP1 has a higher specific activity than CMMP8 under our experimental conditions (as measured against a thiopeptolide substrate; see Materials and Methods), it degrades collagen with considerably lower efficiency than CMMP8 (Figure 2). To decipher the physical basis for this reduced activity, we applied the reaction scheme shown in Figure 4 to the CMMP1 degradation experiments.

Given that K_{eq} is an inherent property of type I collagen at a given temperature and both CMMP1 and CMMP8 collagen degradation experiments were performed at room temperature, K_{eq} is the same for both reactions. Thus, we used our degradation model to determine the range of $(K^{VC}_{bind})_{CMMP1}$. As k_{cat} corresponds to the catalytic rate once the protein has bound the vulnerable state (that is unfolded in the region of the scissile bond), it is estimated using previously determined k_{cat} values for MMP1 degrading gelatin from type I collagen (Table S3, Supporting Information) (*46*).

With $K_{eq} = (1.7-2.1) \times 10^{-3}$, the best fits are found for $(K^{VC}_{bind})_{CMMP1} = (0.9-1.3) \times 10^4$ M^{-1} (Figure 7). These data suggest that CMMP1's binding affinity for the vulnerable state of collagen is nearly 2 orders of magnitude lower than that of CMMP8. Expressed as a difference of binding free energies, $\Delta\Delta G_{bind} = (\Delta G_{bind})_{CMMP1} - (\Delta G_{bind})_{CMMP8}$, the binding of CMMP1 to type I collagen is approximately 2.5 kcal/mol less favorable than the binding of CMMP8 to type I collagen.

DISCUSSION

Our results unambiguously demonstrate that collagenolysis can occur with MMP deletion mutants that contain only the catalytic domain and therefore indicate that the hemopexin-like domain is not required for peptide bond hydrolysis and enzyme specificity at room temperature. Moreover, while both CMMP1 and CMMP8 cleave completely unfolded type I collagen chains at multiple sites, both enzymes cleave type I collagen *in vitro* at only one site that corresponds to the unique cleavage site recognized by full-length collagenases. In light of these observations we interpret our results using a conformational selection model where thermal fluctuations at the unique cleavage site cause the protein to sample partially unfolded vulnerable states that can then be recognized and cleaved by collagenases (*21*). This formalism allows us to estimate the relative amounts of native and vulnerable states at room temperature from an analysis of type I collagen degradation data. Estimates of K_{eq} for a small heterotrimeric peptide modeling the collagenase cleavage site in type I collagen suggest that the vulnerable state dominates at room temperature for this peptide, a finding in agreement with the measured melting temperature of this peptide (*45*). For type I collagen at room temperature the calculated K_{eq} of $(1.7-2.1) \times 10^{-3}$ corresponds to a free energy difference of ~3.5 kcal/mol between the two states, where the folded triple-helical state is the most stable. This free energy difference corresponds to breaking two to four favorable hydrogen bonds, a finding in agreement with a previously proposed structure of the type I collagen vulnerable state (*27*). Interestingly, this estimate for the relative amounts of vulnerable states for both the scissile bond-containing heterotrimeric peptide and type I collagen in solution was obtained from an analysis of the degradation data alone. That is, although the model itself does not explicitly contain information about the temperature at which the experiments were performed, it correctly predicts that the degradation experiments were performed at a relatively high temperature for the heterotrimeric peptide and a relatively low temperature for collagen.

Previous experiments that incubated type I collagen with deletion mutants corresponding to the catalytic domain of MMPs failed to discover any degradation products, thereby suggesting that collagen does not adopt partially unfolded conformations at room temperature (*19*, *30*). However, as our work demonstrates, at temperatures well below collagen's melting temperature, the relative concentration of partially unfolded conformers will be small, and consequently the rate of collagen degradation will be low (*21*). Under these conditions appreciable amounts of degradation will only be observed when relatively

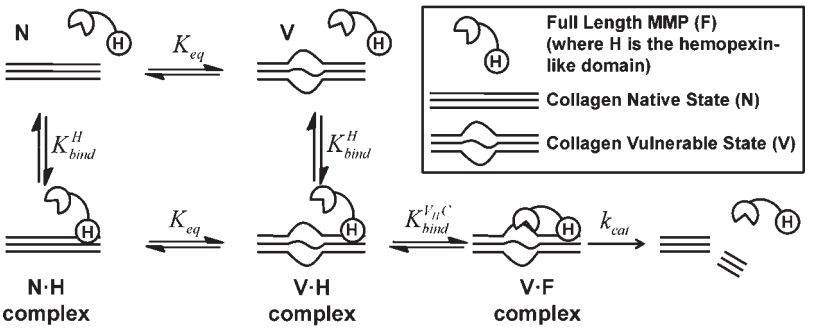

FIGURE 8: A conformational selection mechanism for collagenolysis with full-length collagenases. Collagen exists in an equilibrium between native (N) and vulnerable (V) states determined by the equilibrium constant K_{eq}. Full-length MMP (F) can bind to the native state of collagen via the hemopexin-like domain (H) with binding constant K^{H}_{bind}, forming the N·H complex. The N·H complex can transition to the V·H complex via the equilibrium between native and vulnerable states, K_{eq}. The full-length enzyme, F, can bind directly to the vulnerable state, V, via the hemopexin domain (H) forming the V·H complex, again determined by the binding constant K^{H}_{bind}. Once a V·H complex is formed, the catalytic domain of the full-length MMP can bind to the vulnerable state with a binding constant $K^{V_H C}_{bind}$, forming the V·F complex. The V·F complex is then degraded with catalytic rate k_{cat}.

long incubation times are used. More precisely, we find that 2 days of incubation time with CMMP8 and 6 days with CMMP1 are required to see evidence of collagen degradation.

Additionally, our results offer an explanation for the different type I collagen efficiencies of CMMP1 and CMMP8. While the catalytic rates for the two enzymes are likely different, our data suggest that variations in k_{cat} are insufficient to explain the differences in the overall degradation rates. On the other hand, we find that the binding of CMMP1 to the vulnerable state of type I collagen is 2.5 kcal/mol less favorable than the binding of CMMP8. This free energy difference corresponds to relatively small differences in the bound structures themselves; e.g., breaking one to two favorable hydrogen bonds could easily explain a difference of this magnitude. Together, these data suggest that subtle changes in binding between similar homologous enzymes can lead to significant differences in the overall reaction kinetics.

Although several potential cleavage sites exist in collagen, only one unique site is cleaved by MMPs (*14*, *23*, *24*). Recent observations suggest that cleavage site specificity is mediated by interactions of noncatalytic domains with distinct sites on collagen and that these interactions may play an important role in enzyme specificity (*33*, *62*). Since we find that cleavage at the unique collagenase cleavage site is achieved using deletion mutants of MMP1 and MMP8 that lack the noncatalytic hemopexin-like domains, these noncatalytic domains are not required for cleavage site specificity *in vitro* at room temperature. Theoretical studies and experiments on collagen-like model peptides both suggest that the region near the collagenase cleavage site has a relatively low stability (*20*, *22*, *26*, *27*, *63*, *64*). This decreased stability ensures that the cleavage site preferentially unfolds at low temperatures, thereby ensuring that the scissile bond is recognized by MMP catalytic domains.

The physical basis underlying the decreased stability of regions in the vicinity of the collagenase cleavage site has been explored in a variety of different studies. An analysis of collagen sequences from different species suggests that regions near the collagenase cleavage sites have a relative paucity of imino acids (Pro and Hyp) (*14*). Since Pro and Hyp content is related to triple-helical stability, the relative lack of these residues is a contributing factor to the decreased stability of these regions (*65*, *66*). Additional studies suggest it is not just the reduced imino acid content that is responsible for the decreased stability of these regions and that the precise amino acid sequence about these regions imparts increased conformational flexibility in these regions (*20*, *22*, *27*).

Our data are explained by the fact that the unique scissile bond locally unfolds at low temperatures. However, as the temperature increases, microunfolding of collagen leads to the exposure of other potential cleavage sites that can be recognized by MMP deletion mutants (*67*). Indeed, recent data suggest that collagen is thermally unstable at body temperature, and it has been postulated that microunfolding of distinct collagen regions facilitates fibril formation and collagen catabolism (*51*). As the MMP hemopexin-like domain has binding sites near the collagenase cleavage site, it may help to localize the enzyme to a specific scissile bond, thereby ensuring that the correct site is cleaved at body temperature (*33*). Therefore, while our data argue that the hemopexin-like domain is not needed for cleavage site specificity at low temperatures, it may play an important role in determining specificity at body temperature.

In light of these considerations we expand our previous reaction scheme for the catalytic domain alone to consider the effects of the hemopexin-like domain on collagenolysis (Figure 8). In this reaction scheme, collagen exists in an equilibrium between native (N) and vulnerable (V) states, and either state can be bound by collagenases via the hemopexin-like domain, which contains binding sites for collagen (*13*, *32*, *33*, *68*, *69*). When the native state is bound, an N·H complex is formed that cannot be cleaved since the scissile bond in this structure is not accessible to the MMP active site. Since the catalytic domain of the enzyme is not bound to the scissile bond in the N·H complex and the putative binding site for the hemopexin-like domain in type I collagen is removed from the cleavage site (*33*, *62*), the N·H complex can transition to a vulnerable state (V·H complex) via a conformational change similar to the one experienced by unbound collagen. Once the V·H complex is formed, the catalytic domain can then bind the accessible scissile bond, yielding the V·F complex, which then goes on to form degraded protein.

To understand how the presence of enzyme might affect the relative concentration of vulnerable states, we consider an equilibrium in which the enzyme is catalytically inactive (i.e., the degradation step does not occur) and solve for the effective ratio of all vulnerable states to all native states, $K^{eff}_{eq} = ([V] + [V \cdot H] +$

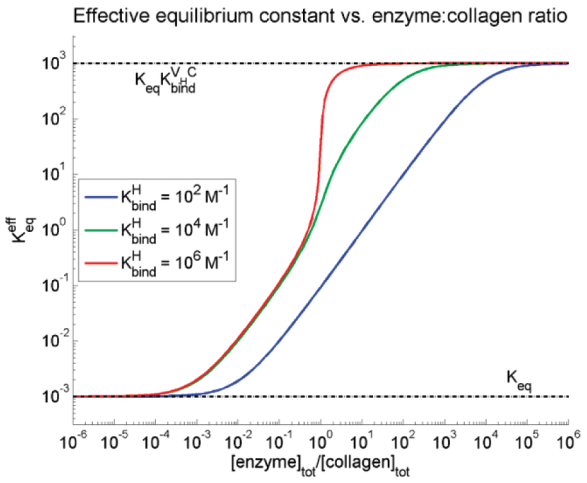

FIGURE 9: Change in the effective conformational equilibrium of collagen in the presence of full-length collagenase. Computed values for the effective equilibrium constant, K_{eq}^{eff}, as a function of total enzyme-to-collagen ratio for three possible values of the hemopexin-like domain binding constant, K_{bind}^{H}, ranging from submillimolar to micromolar affinity. For these calculations, $[collagen]_{tot} = 10^{-6}$ M, $K_{eq} = 10^{-3}$, and $K_{bind}^{V_HC} = 10^6$. At low enzyme-to-collagen ratios, K_{eq}^{eff} is approximately equal to K_{eq}, whereas at high enzyme-to-collagen ratios, K_{eq}^{eff} approaches $K_{eq}K_{bind}^{V_HC}$.

$[V\cdot F])/([N] + [N\cdot H])$. In this scenario, there is a closed form solution for K_{eq}^{eff}:

$$K_{eq}^{eff} = K_{eq}\left(1 + \left(\frac{K_{bind}^{H}[E]}{1 + K_{bind}^{H}[E]}\right)K_{bind}^{V_HC}\right) \quad (7)$$

where [E] is the concentration of free enzyme, which itself is a function of the enzyme-to-substrate ratio and the binding constants K_{bind}^{H} and $K_{bind}^{V_HC}$. We can better understand the behavior of K_{eq}^{eff} by evaluating it at two limiting conditions. In the first, no enzyme is present ($[E] = [E]_{tot} = 0$) and/or the enzyme does not bind collagen ($K_{bind}^{H} = 0$); in either case $K_{eq}^{eff} = K_{eq}$. The second limiting condition is when the concentration of enzyme is in relative excess and K_{bind}^{H} is nonzero; in this case, $K_{eq}^{eff} \approx K_{eq}(1 + K_{eq}K_{bind}^{V_HC})$. Given that the catalytic domain is restricted to reside in the vicinity of the cleavage site when the hemopexin-like domain is bound, the entropic loss upon binding of the catalytic domain is relatively small when the enzyme is anchored to the protein by the hemopexin-like domain. Consequently, we expect that $K_{bind}^{V_HC} \gg 1$ and therefore that $K_{eq}^{eff} \approx K_{eq}K_{bind}^{V_HC}$. Accordingly, this suggests that as long as there is a nonzero total concentration of enzyme, we will have $K_{eq} < K_{eq}^{eff} < K_{eq}K_{bind}^{V_HC}$, as demonstrated in Figure 9. In other words, the ratio of vulnerable states to native states, K_{eq}^{eff}, will always be greater than K_{eq} when enzyme is present simply due to the principle of mass action. In this way the presence of enzyme leads to an effective increase in the concentration of vulnerable, "unwound", conformers without requiring energy input or active enzyme-mediated unwinding.

Our formalism analyzes the degradation of collagen in solution by means of both experimental and numerical studies, but *in vivo* collagen typically exists in a fibrillar state (*2*). Since previous studies suggest that type I collagen is thermally stabilized in a fibrillar context relative to the solution state, it is an open question as to whether the conformational ensemble of the collagenase cleavage site is the same in the fibril as it is in solution (*70*). Hence, at any given temperature, K_{eq} will be smaller for a collagen molecule located in a fibril relative to the same molecule free in solution. Interestingly, recent fiber diffraction studies suggest that the α2(I) chain is relatively dissociated from the central axis of the helix at the collagenase cleavage site *in situ*; i.e., in the fibrillar state, the triple helix is disrupted near the cleavage site (*33*). While the fiber diffraction study is of insufficient resolution to provide reliable details on the atomic structure of the fibrillar state, these data do suggest that triple-helical stability can vary considerably along its length and especially near the collagenase cleavage site. Thus, while *in vivo* collagen degradation clearly differs from the solution state degradation studies presented in this work, the mechanism outlined in Figure 8 and the preceding discussion may still be a fair representation of the important aspects of *in vivo* collagen degradation; albeit the value of K_{eq} is likely much smaller in the fibrillar context.

Methods designed to prevent excessive collagen degradation in disorders of collagen metabolism have mainly focused on designing small molecule inhibitors of the MMP active site that would prevent binding and hydrolysis of the scissile bond (*71*, *72*). This corresponds to disrupting the reaction step involving the transition between the V·H and V·F complexes in Figure 8. Although great effort has been directed toward the design of such inhibitors, selectivity issues and secondary side effects in clinical trials have been encountered, and therefore only few inhibitors have been made available commercially (*72*−*75*). The reaction scheme in Figure 8 highlights additional and potentially fruitful avenues for abrogating disease-associated collagenolysis. As others have noted, disruption of hemopexin-like domain binding to secondary sites on collagen could prove to be an effective mechanism to modulate collagenolysis (e.g., decreasing K_{bind}^{H}) (*10*, *68*, *71*). Our data suggest that mechanisms that lead to stabilization of the native state relative to the vulnerable state (i.e., decreasing K_{eq}) may have a similar desirable effect. By utilizing these additional steps in the reaction mechanism, collagen degradation could potentially be inhibited in a specific and efficient manner.

Overall, our data are consistent with the notion that the conformational ensemble of type I collagen includes locally unfolded conformations that have relatively exposed scissile bonds, even at temperatures below the protein's melting temperature. These locally unfolded conformations are the basis of a conformational selection mechanism in which collagenases recognize and cleave these preexisting locally unfolded states. This degradation mechanism presents a framework both for understanding the basic interaction of collagen with collagenases and for therapeutic strategies to modulate excessive collagenolysis associated with many diseases.

ACKNOWLEDGMENT

We thank William M. Wyatt, Steven J. Pennybaker, and Dr. Sophie Walker for help with the degradation experiments.

SUPPORTING INFORMATION AVAILABLE

A list of parameter values used in the numerical simulations and additional figures referenced in this work showing the RMSEs of fits for degradation experiments involving CMMP8 (using different values of k_{cat}) as well as a derivation of the effective equilibrium constant in the presence of full-length enzyme. This material is available free of charge via the Internet at http://pubs.acs.org.

REFERENCES

1. Hohenester, E., and Engel, J. (2002) Domain structure and organisation in extracellular matrix proteins. *Matrix Biol. 21*, 115–128.
2. Gelse, K., Poschl, E., and Aigner, T. (2003) Collagens—structure, function, and biosynthesis. *Adv. Drug Deliv. Rev. 55*, 1531–1546.

3. Bella, J., Eaton, M., Brodsky, B., and Berman, H. M. (1994) Crystal and molecular structure of a collagen-like peptide at 1.9 Å resolution. *Science 266*, 75–81.
4. Ramachandran, G. N., and Kartha, G. (1955) Structure of collagen. *Nature 176*, 593–595.
5. Rich, A., and Crick, F. H. (1961) The molecular structure of collagen. *J. Mol. Biol. 3*, 483–506.
6. Barnes, M. J., and Farndale, R. W. (1999) Collagens and atherosclerosis. *Exp. Gerontol. 34*, 513–525.
7. Bode, M. K., Mosorin, M., Satta, J., Risteli, L., Juvonen, T., and Risteli, J. (1999) Complete processing of type III collagen in atherosclerotic plaques. *Arterioscler., Thromb., Vasc. Biol. 19*, 1506–1511.
8. Celentano, D. C., and Frishman, W. H. (1997) Matrix metalloproteinases and coronary artery disease: a novel therapeutic target. *J. Clin. Pharmacol. 37*, 991–1000.
9. McDonnell, S., Morgan, M., and Lynch, C. (1999) Role of matrix metalloproteinases in normal and disease processes. *Biochem. Soc. Trans. 27*, 734–740.
10. Nerenberg, P. S., Salsas-Escat, R., and Stultz, C. M. (2007) Collagen—a necessary accomplice in the metastatic process. *Cancer Genomics Proteomics 4*, 319–328.
11. Libby, P. (2008) The molecular mechanisms of the thrombotic complications of atherosclerosis. *J. Intern. Med. 263*, 517–527.
12. Bode, W., Fernandez-Catalan, C., Tschesche, H., Grams, F., Nagase, H., and Maskos, K. (1999) Structural properties of matrix metalloproteinases. *Cell. Mol. Life Sci. 55*, 639–652.
13. Overall, C. M. (2002) Molecular determinants of metalloproteinase substrate specificity: matrix metalloproteinase substrate binding domains, modules, and exosites. *Mol. Biotechnol. 22*, 51–86.
14. Fields, G. B. (1991) A model for interstitial collagen catabolism by mammalian collagenases. *J. Theor. Biol. 153*, 585–602.
15. Conway, J. G., Wakefield, J. A., Brown, R. H., Marron, B. E., Sekut, L., Stimpson, S. A., McElroy, A., Menius, J. A., Jeffreys, J. J., and Clark, R. L.; et al. (1995) Inhibition of cartilage and bone destruction in adjuvant arthritis in the rat by a matrix metalloproteinase inhibitor. *J. Exp. Med. 182*, 449–457.
16. Cowan, K. N., Jones, P. L., and Rabinovitch, M. (2000) Elastase and matrix metalloproteinase inhibitors induce regression, and tenascin-C antisense prevents progression, of vascular disease. *J. Clin. Invest. 105*, 21–34.
17. Di Sebastiano, P., di Mola, F. F., Artese, L., Rossi, C., Mascetta, G., Pernthaler, H., and Innocenti, P. (2001) Beneficial effects of Batimastat (BB-94), a matrix metalloproteinase inhibitor, in rat experimental colitis. *Digestion 63*, 234–239.
18. Peterson, J. T., Hallak, H., Johnson, L., Li, H., O'Brien, P. M., Sliskovic, D. R., Bocan, T. M., Coker, M. L., Etoh, T., and Spinale, F. G. (2001) Matrix metalloproteinase inhibition attenuates left ventricular remodeling and dysfunction in a rat model of progressive heart failure. *Circulation 103*, 2303–2309.
19. Chung, L., Dinakarpandian, D., Yoshida, N., Lauer-Fields, J. L., Fields, G. B., Visse, R., and Nagase, H. (2004) Collagenase unwinds triple-helical collagen prior to peptide bond hydrolysis. *EMBO J. 23*, 3020–3030.
20. Stultz, C. M. (2002) Localized unfolding of collagen explains collagenase cleavage near imino-poor sites. *J. Mol. Biol. 319*, 997–1003.
21. Nerenberg, P. S., Salsas-Escat, R., and Stultz, C. M. (2008) Do collagenases unwind triple-helical collagen before peptide bond hydrolysis? Reinterpreting experimental observations with mathematical models. *Proteins 70*, 1154–1161.
22. Salsas-Escat, R., and Stultz, C. M. (2009) Conformational selection and collagenolysis in type III collagen. *Proteins 78*, 325–335.
23. Kuivaniemi, H., Tromp, G., Chu, M. L., and Prockop, D. J. (1988) Structure of a full-length cDNA clone for the prepro alpha 2(I) chain of human type I procollagen. Comparison with the chicken gene confirms unusual patterns of gene conservation. *Biochem. J. 252*, 633–640.
24. Tromp, G., Kuivaniemi, H., Stacey, A., Shikata, H., Baldwin, C. T., Jaenisch, R., and Prockop, D. J. (1988) Structure of a full-length cDNA clone for the prepro alpha 1(I) chain of human type I procollagen. *Biochem. J. 253*, 919–922.
25. Makareeva, E., Mertz, E. L., Kuznetsova, N. V., Sutter, M. B., DeRidder, A. M., Cabral, W. A., Barnes, A. M., McBride, D. J., Marini, J. C., and Leikin, S. (2008) Structural heterogeneity of type I collagen triple helix and its role in osteogenesis imperfecta. *J. Biol. Chem. 283*, 4787–4798.
26. Fiori, S., Sacca, B., and Moroder, L. (2002) Structural properties of a collagenous heterotrimer that mimics the collagenase cleavage site of collagen type I. *J. Mol. Biol. 319*, 1235–1242.
27. Nerenberg, P. S., and Stultz, C. M. (2008) Differential unfolding of alpha1 and alpha2 chains in type I collagen and collagenolysis. *J. Mol. Biol. 382*, 246–256.
28. Bruckner, P., and Prockop, D. J. (1981) Proteolytic enzymes as probes for the triple-helical conformation of procollagen. *Anal. Biochem. 110*, 360–368.
29. Miller, E. J., Finch, J. E., Jr., Chung, E., Butler, W. T., and Robertson, P. B. (1976) Specific cleavage of the native type III collagen molecule with trypsin. Similarity of the cleavage products to collagenase-produced fragments and primary structure at the cleavage site. *Arch. Biochem. Biophys. 173*, 631–637.
30. Schnierer, S., Kleine, T., Gote, T., Hillemann, A., Knauper, V., and Tschesche, H. (1993) The recombinant catalytic domain of human neutrophil collagenase lacks type I collagen substrate specificity. *Biochem. Biophys. Res. Commun. 191*, 319–326.
31. Gioia, M., Monaco, S., Fasciglione, G. F., Coletti, A., Modesti, A., Marini, S., and Coletta, M. (2007) Characterization of the mechanisms by which gelatinase A, neutrophil collagenase, and membrane-type metalloproteinase MMP-14 recognize collagen I and enzymatically process the two alpha-chains. *J. Mol. Biol. 368*, 1101–1113.
32. Tam, E. M., Moore, T. R., Butler, G. S., and Overall, C. M. (2004) Characterization of the distinct collagen binding, helicase and cleavage mechanisms of matrix metalloproteinase 2 and 14 (gelatinase A and MT1-MMP): the differential roles of the MMP hemopexin c domains and the MMP-2 fibronectin type II modules in collagen triple helicase activities. *J. Biol. Chem. 279*, 43336–43344.
33. Perumal, S., Antipova, O., and Orgel, J. P. (2008) Collagen fibril architecture, domain organization, and triple-helical conformation govern its proteolysis. *Proc. Natl. Acad. Sci. U.S.A. 105*, 2824–2829.
34. Epstein, E. H., Jr. (1974) (Alpha1(3))3 human skin collagen. Release by pepsin digestion and preponderance in fetal life. *J. Biol. Chem. 249*, 3225–3231.
35. Miller, E. J., and Rhodes, R. K. (1982) Preparation and characterization of collagens, in Methods in Enzymology Vol. 82, Structural and Contractile Proteins, Part A Extracellular Matrix (Cunningham, L. W., and Fredericksen, D. W., Eds.) pp 41−44, Academic Press, New York.
36. Trelstad, R. L., Catanese, V. M., and Rubin, D. F. (1976) Collagen fractionation: separation of native types I, II and III by differential precipitation. *Anal. Biochem. 71*, 114–118.
37. Weingarten, H., and Feder, J. (1985) Spectrophotometric assay for vertebrate collagenase. *Anal. Biochem. 147*, 437–440.
38. Weingarten, H., Martin, R., and Feder, J. (1985) Synthetic substrates of vertebrate collagenase. *Biochemistry 24*, 6730–6734.
39. Kadler, K. E., Hojima, Y., and Prockop, D. J. (1987) Assembly of collagen fibrils de novo by cleavage of the type I pC-collagen with procollagen C-proteinase. Assay of critical concentration demonstrates that collagen self-assembly is a classical example of an entropy-driven process. *J. Biol. Chem. 262*, 15696–15701.
40. Knäuper, V., and Murphy, G. (2001) Methods for studying activation of matrix metalloproteinases, in Matrix Metalloproteinase Protocols (Clark, I. M., Ed.) pp 377−387, Humana Press, Totowa, NJ.
41. French, M. F., Mookhtiar, K. A., and Van Wart, H. E. (1987) Limited proteolysis of type I collagen at hyperreactive sites by class I and II *Clostridium histolyticum* collagenases: complementary digestion patterns. *Biochemistry 26*, 681–687.
42. Morimoto, K., Kawabata, K., Kunii, S., Hamano, K., Saito, T., and Tonomura, B. (2009) Characterization of type I collagen fibril formation using thioflavin T fluorescent dye. *J. Biochem. 145*, 677–684.
43. Shigemura, Y., Ando, M., Harada, K., and Tsukamasa, Y. (2004) Possible degradation of type I collagen in relation to yellowtail muscle softening during chilled storage. *Fish. Sci. 70*, 703–709.
44. Veis, A., and Anesey, J. (1965) Modes of intermolecular cross-linking in mature insoluble collagen. *J. Biol. Chem. 240*, 3899–3908.
45. Ottl, J., Gabriel, D., Murphy, G., Knauper, V., Tominaga, Y., Nagase, H., Kroger, M., Tschesche, H., Bode, W., and Moroder, L. (2000) Recognition and catabolism of synthetic heterotrimeric collagen peptides by matrix metalloproteinases. *Chem. Biol. 7*, 119–132.
46. Welgus, H. G., Jeffrey, J. J., Stricklin, G. P., and Eisen, A. Z. (1982) The gelatinolytic activity of human skin fibroblast collagenase. *J. Biol. Chem. 257*, 11534–11539.
47. Gioia, M., Fasciglione, G. F., Marini, S., D'Alessio, S., De Sanctis, G., Diekmann, O., Pieper, M., Politi, V., Tschesche, H., and Coletta, M. (2002) Modulation of the catalytic activity of neutrophil collagenase MMP-8 on bovine collagen I. Role of the activation cleavage and of the hemopexin-like domain. *J. Biol. Chem. 277*, 23123–23130.
48. Netzel-Arnett, S., Fields, G. B., Birkedal-Hansen, H., and Van Wart, H. E. (1991) Sequence specificities of human fibroblast and neutrophil collagenases. *J. Biol. Chem. 266*, 6747–6755.

49. Wittung-Stafshede, P., Lee, J. C., Winkler, J. R., and Gray, H. B. (1999) Cytochrome *b*(562) folding triggered by electron transfer: Approaching the speed limit for formation of a four-helix-bundle protein. *Proc. Natl. Acad. Sci. U.S.A. 96*, 6587–6590.
50. Kubelka, J., Chiu, T. K., Davies, D. R., Eaton, W. A., and Hofrichter, J. (2006) Sub-microsecond protein folding. *J. Mol. Biol. 359*, 546–553.
51. Leikina, E., Mertts, M. V., Kuznetsova, N., and Leikin, S. (2002) Type I collagen is thermally unstable at body temperature. *Proc. Natl. Acad. Sci. U.S.A. 99*, 1314–1318.
52. Privalov, P. L. (1982) Stability of proteins. Proteins which do not present a single cooperative system. *Adv. Protein Chem. 35*, 1–104.
53. Fietzek, P. P., and Kuhn, K. (1975) The covalent structure of collagen: amino-acid sequence of the cyanogen-bromide peptides alpha1-CB2, alpha1-CB4 and alpha1-CB5 from calf-skin collagen. *Eur. J. Biochem. 52*, 77–82.
54. Fietzek, P. P., Rexrodt, F. W., Hopper, K. E., and Kuhn, K. (1973) The covalent structure of collagen. 2. The amino-acid sequence of alpha1-CB7 from calf-skin collagen. *Eur. J. Biochem. 38*, 396–400.
55. Fietzek, P. P., Rexrodt, F. W., Wendt, P., Stark, M., and Kuhn, K. (1972) The covalent structure of collagen. Amino-acid sequence of peptide 1-CB6-C2. *Eur. J. Biochem. 30*, 163–168.
56. Fietzek, P. P., Wendt, P., Kell, I., and Kuhn, K. (1972) The covalent structure of collagen: amino acid sequence of 1-CB3 from calf skin collagen. *FEBS Lett. 26*, 74–76.
57. Rauterberg, J., Fietzek, P., Rexrodt, F., Becker, U., Stark, M., and Kuhn, K. (1972) The amino acid sequence of the carboxyterminal nonhelical cross link region of the alpha 1 chain of calf skin collagen. *FEBS Lett. 21*, 75–79.
58. Shirai, T., Hattori, S., Sakaguchi, M., Inouye, S., Kimura, A., Ebihara, T., Irie, S., Nagai, Y., and Hori, H. (1998) The complete cDNA coding sequence for the bovine proalpha2(I) chain of type I procollagen. *Matrix Biol. 17*, 85–88.
59. Wendt, P., von der Mark, K., Rexrodt, F., and Kuhn, K. (1972) The covalent structure of collagen. The amino-acid sequence of the 112-residues. Amino-terminal part of peptide 1-CB6 from calf-skin collagen. *Eur. J. Biochem. 30*, 169–183.
60. Gendron, R., Grenier, D., Sorsa, T., and Mayrand, D. (1999) Inhibition of the activities of matrix metalloproteinases 2, 8, and 9 by chlorhexidine. *Clin. Diagn. Lab. Immunol. 6*, 437–439.
61. Courts, A. (1955) The N-terminal amino acid residues of gelatin. 3. Enzymic degradation. *Biochem. J. 59*, 382–386.
62. Erat, M. C., Slatter, D. A., Lowe, E. D., Millard, C. J., Farndale, R. W., Campbell, I. D., and Vakonakis, I. (2009) Identification and structural analysis of type I collagen sites in complex with fibronectin fragments. *Proc. Natl. Acad. Sci. U.S.A. 106*, 4195–4200.
63. Fields, G. B., Van Wart, H. E., and Birkedal-Hansen, H. (1987) Sequence specificity of human skin fibroblast collagenase. Evidence for the role of collagen structure in determining the collagenase cleavage site. *J. Biol. Chem. 262*, 6221–6226.
64. Fan, P., Li, M. H., Brodsky, B., and Baum, J. (1993) Backbone dynamics of $(Pro\text{-}Hyp\text{-}Gly)_{10}$ and a designed collagen-like triple-helical peptide by ^{15}N NMR relaxation and hydrogen-exchange measurements. *Biochemistry 32*, 13299–13309.
65. Brodsky, B., and Persikov, A. V. (2005) Molecular structure of the collagen triple helix. *Adv. Protein Chem. 70*, 301–339.
66. Persikov, A. V., Ramshaw, J. A., and Brodsky, B. (2005) Prediction of collagen stability from amino acid sequence. *J. Biol. Chem. 280*, 19343–19349.
67. Taddese, S., Jung, M. C., Ihling, C., Heinz, A., Neubert, R. H., and Schmelzer, C. E. (2009) MMP-12 catalytic domain recognizes and cleaves at multiple sites in human skin collagen type I and type III. *Biochim. Biophys. Acta 1803*, 20–28.
68. Lauer-Fields, J. L., Chalmers, M. J., Busby, S. A., Minond, D., Griffin, P. R., and Fields, G. B. (2009) Identification of specific hemopexin-like domain residues that facilitate matrix metalloproteinase collagenolytic activity. *J. Biol. Chem. 284*, 24017–24024.
69. Murphy, G., Allan, J. A., Willenbrock, F., Cockett, M. I., O'Connell, J. P., and Docherty, A. J. (1992) The role of the C-terminal domain in collagenase and stromelysin specificity. *J. Biol. Chem. 267*, 9612–9618.
70. Birkedal-Hansen, H., Taylor, R. E., Bhown, A. S., Katz, J., Lin, H. Y., and Wells, B. R. (1985) Cleavage of bovine skin type III collagen by proteolytic enzymes. Relative resistance of the fibrillar form. *J. Biol. Chem. 260*, 16411–16417.
71. Folgueras, A. R., Pendas, A. M., Sanchez, L. M., and Lopez-Otin, C. (2004) Matrix metalloproteinases in cancer: from new functions to improved inhibition strategies. *Int. J. Dev. Biol. 48*, 411–424.
72. Georgiadis, D., and Yiotakis, A. (2008) Specific targeting of metzincin family members with small-molecule inhibitors: progress toward a multifarious challenge. *Bioorg. Med. Chem. 16*, 8781–8794.
73. Abbenante, G., and Fairlie, D. P. (2005) Protease inhibitors in the clinic. *Med. Chem. 1*, 71–104.
74. Ganea, E., Trifan, M., Laslo, A. C., Putina, G., and Cristescu, C. (2007) Matrix metalloproteinases: useful and deleterious. *Biochem. Soc. Trans. 35*, 689–691.
75. Tallant, C., Marrero, A., and Gomis-Ruth, F. X. (2009) Matrix metalloproteinases: fold and function of their catalytic domains. *Biochim. Biophys. Acta 1803*, 20–28.